
Analysis Of Human Femur Bone At Different Orientation Under Three Point Bending Load Using Fea

S. MATHU KUMAR^{1*}, V.A. NAGARAJAN², A. RADHAKRISHNAN³, RAMANAN A⁴

¹*Department of Mechanical Engineering, Ponjesly college of Engineering, Nagercoil, India.*

²*Department of Mechanical Engineering, University college of Engineering, Nagercoil, India.*

³*Department of Information Technology, University college of Engineering, Nagercoil, India.*

⁴*Scientific Officer, TNSCST, Chennai, Tamil Nadu, India.*

**Correspondence to S. MATHU KUMAR.*

Abstract

The femur bone is the human body's largest and strongest bone. If this bone is affected in any accident, the injured person will be paralyzed. This work describes the fracture morphology of femur bone derived from the loading mechanisms of bending at various orientations over the femur bone. The maximum strain and displacement were determined using a finite element (FE) analysis, which was highly dependent on the precision of the recorded geometry and appropriate assignment of material properties. In this research, FE analysis was performed in a tantom three-point bending test. In actual life, loading cannot always be expected in a fixed direction. Here, the load was applied at the middle of the bone at eight different orientations, 45° apart. Maximum strain, displacement, and orientation over the femur bone were identified by this analysis.

Key words: Femur bone, FEA, Biomechanics, Three Point bending Analysis, Strain

INTRODUCTION

The biomechanical behavior of human bones has created the curiosity of scientists and physicians, particularly the femur bone, which is the largest and strongest bone in the body. In the existing experimental analysis, 2D and, 3D geometries as well as homogeneous, elastic, and isotropic properties [1-3] have been discussed. In recent experiments, computer aided design and CT scanning have been used to represent geometries. Furthermore, the appropriate material properties of human bones have been considered [4-6, 23]. The fracture load of bones has been accurately predicted using quantitative computed tomography (QCT) based FE models under diverse loading circumstances [7-8]. The FE analysis produces a high error while providing inaccurate material properties [9-10], geometry and boundary conditions.

The most common fracture faced by humans is proximal femoral fracture, which cripples the injured person throughout their life [11]. In general; FE is one of the strongest tools for predicting the failure of biological composites. It is also useful in predicting human

bone failure too¹⁶⁻¹⁷. An analysis was carried out to investigate the impact of strain rate on the mechanical properties of bone.

In most of the previous studies and analysis, the load or force was applied in the 180° loading position [12]. Here, the applied load is considered to be 180° in the standing posture of the human body. However, in actual life, the load may be from any direction. In our research, eight directions (orientation) were analyzed, discussed, and predicted. The different chances of the load direction are shown in Figure 1.

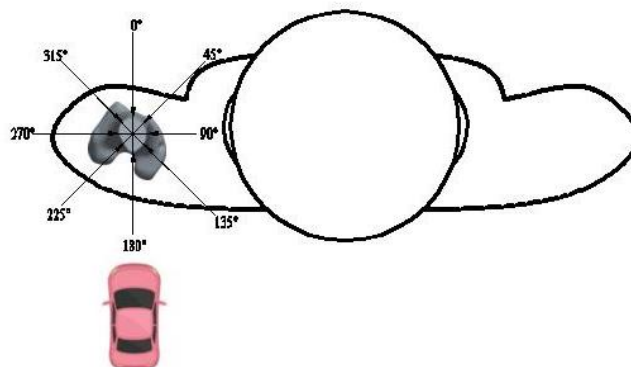


Figure1. Different chances of load direction

MATERIALS AND METHODS

2.1 Reconstruction of the FE model

High-resolution computed tomography images were used for proximal femur specimens. The 3D Doctor software was used to reconstruct the femur bone model from the CT scan images. The reconstructed file was exported to the CREO software and converted to the ACIS format. This format enhances the results of femur bone analysis using the ANSYS software. Linear tetrahedral elements were used in this study. This is because it provides a smooth surface for the model [18]. Based on the previous analysis the material properties were taken and the same were assigned to the femur bone [19-21].

2.2 FE analysis

The position of the strain gauge on the surface of the femur bone was 180° apart from the center loading point of the three-point analysis (TPBA), which is 50% of the distance from the proximal end. The FE model was subjected to boundary and loading conditions, as shown in the existing TPBA. For TPBA, the supports were located at the distal and proximal ends. Here the axes are constrained vertically downward alone [15, 21-23].

At the middle, in between the supports, a vertical downward point load is applied which varies from 100 to 1000N with the increment of 100N. Strain values were recorded

against the corresponding loads. The load and strain increased linearly. The point load is applied repeatedly on the same position of the femur bone by rotating it at 45° steps in a clockwise direction at each time. This procedure was repeated eight times to complete 360°. The direction of the applied load, on the femur bone is shown in Figure 2.

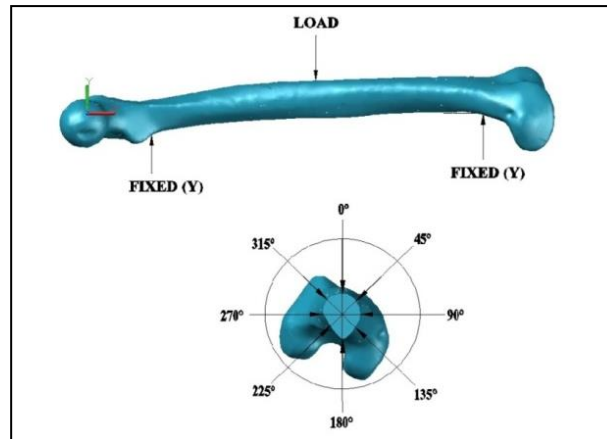


Figure 2. Direction of load applied on the femur bone

The minimum strain occurred in the 135° orientation at 100 N load, and the minimum displacement occurred in the 0° orientation at 100 N load. The maximum strain and maximum displacement occurred on the 270° at 1000 N load.

RESULT AND DISCUSSION

The results of the FE analysis of femur bone, load vs. strain, and load vs. displacement are shown in Figure 3 and 4, respectively.

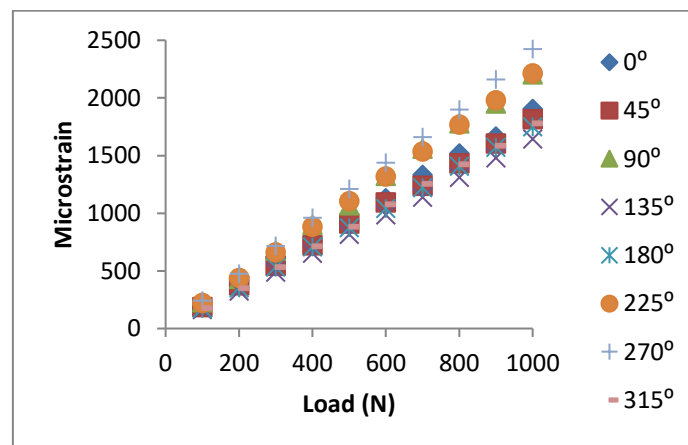


Figure 3. Load vs. strain at all load positions

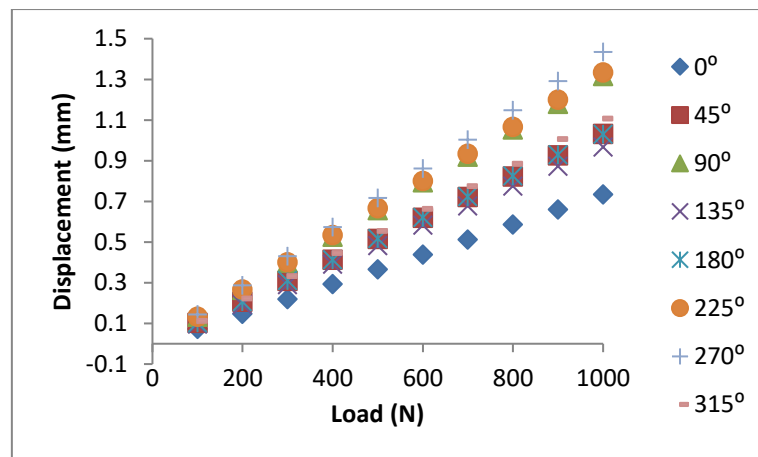


Figure 4. Load vs. displacement at all load positions

From the figures 3 & 4, it is clear that

- For a load of 100N, the minimum strain occurred at the orientation of 135°, and the maximum strain occurred at the orientation of 270°. However, the minimum displacement occurred at an orientation of 0°, and the maximum displacement coincided with the maximum strain orientation.
- For a load of 500N, the minimum strain occurred at the orientation of 135° and the maximum strain occurred at the orientation of 270°, but the minimum displacement occurred at the orientation of 0° and maximum displacement occurred at the orientation of 270°.
- For a load of 1000N, the minimum displacement was obtained from 0° and the minimum strain was obtained from 135° but both the maximum strain and displacement obtained at 270° orientation of the femur bone.

For the same force, the strain and displacement varied in a zigzag pattern at different orientations. This is due to changes in the bone profile. The maximum strain and displacement were obtained at the 270° load position because of its lower distance in the cross section of the bone at that position, as shown in Figure 2. When the applied force was increased from 100 to 1000 N, the strain and displacement also increased linearly.

Conclusion

To determine the strain and displacement in each orientation, loads were varied from 100 to 1000 N in different orientations on the femur bone 45° apart. From the analysis, it is clear that the accuracy of the geometry and material properties are highly influencing the performance of the FE model. Above all, the femur bone has neither a uniform cross section

nor a uniform shape throughout the length of bone. Hence, the load-carrying capacity varies in different orientations. The conclusions of the analysis are as follows.

- The analysis so far made in previous studies at an angle of 180° alone was not sufficient for predicting the actual failure.
- The overall minimum strain (164) occurred at 100 N with an orientation of 135° .
- The overall minimum displacement (0.0733 mm) occurred at 100 N with an orientation of 0° .
- The overall maximum strain (2422) and maximum displacement (1.435 mm) occurred at 1000 N with an orientation of 270° .
- From the above, it is concluded that the load and its orientation are equally important for the correct prediction of failure of the femur bone.

REFERENCES

- [1] Valliapan S, Svensson N L and Wood R D. Three Dimensional Stress Analysis of the Human Femur. *Comput. Biol. Med.* 1977; 7:253–264.
- [2] Cheal E J, Hayes W C, White A A and Perren S M. Three Dimensional Finite Element Analysis of a Simplified Compression Plate Fixation System. *J. Biomech. Eng.* 1984; 106:295–301.
- [3] Cheal E J, Hayes W C, White A A and Perren S M. Stress Analysis of Compression Plate Fixation and its Effects on Long Bone Remodeling. *J. Biomech.* 1985;182:141–150.
- [4] Cheung G, Zalzal P, Bhandari M, Spelt J K and Papini M. Finite Element Analysis of a Femoral Retrograde Intramedullary Nail Subject to Gait Loading. *Med. Eng. Phys.* 2004; 26:93–108.
- [5] Cheal E J, Spector M and Hayes W C. Role of Loads and Prosthesis Material Properties on the Mechanics of the Proximal Femur after Total Hip Arthroplasty. *Journal of Orthop. Res.* 1992;10:405–422.
- [6] Wang C J, Yettram A L, Yao M S and Proctor P. Finite Element Analysis of a Gamma Nail Within a Fractured Femur. *Med. Eng. Phys.* 1998;20:677–683.
- [7] Bessho M, Ohnishi I, Matsuyama J, Matsumoto T and Imai K Nakamura. Prediction of strength and strain of the proximal femur by a CT-based finite element method. *J Biomech.* 2007;8:1745–1753.

- [8] Schileo E, Dall'Ara E, Taddei F, Malandrino A, Schotkamp T, Baleani and Viceconti M. An accurate estimation of bone density improves the accuracy of subject specific finite element models. *J Biomech.* 2008;11:2483–2491.
- [9] Taddei F, Cristofolini L, Martelli S, Gill H S and Viceconti M. Subject specific finite element models of long bones: an in vitro evaluation of the overall accuracy. *J Biomech.* 2006;13:2457–2467.
- [10] Schileo E, Taddei F, Malandrino A, Cristofolini L and Viceconti M. Subject specific finite element models can accurately predict strain levels in long bones. *J Biomech.* 2007;13:2982–2989.
- [11] Austman R L, Milner J S, Holdsworth D W and Dunning C E. The effect of the density modulus relationship selected to apply material properties in a finite element model of long bone. *J Biomech.* 2008; 15:3171–3176.
- [12] Bhatia V A, Edwards W B and Troy K L. Predicting surface strains at the human distal radius during an in vivo loading task finite element model validation and application. *J Biomech.* 2014 ; 47(11):2759-2765.
- [13] Frost H M. Bone's mechanostat: a update. *The anatomical record*, 2003; 275(2) : 1081-1101.
- [14] Gross T S, Edwards J L, Mcleod K J and Rubin C T. Strain gradients correlate with sites of periosteal bone formation. *J Bone Miner Res.* 1997; 12 (6):982-988.
- [15] Bino Varghese, David Short, Ravi Penmetsa, Tarun Goswami and Thomas Hangartner. Computed tomography based finite element models of long bones can accurately capture strain response to bending and torsion. *J Biomech.* 2011; 44: 1374–1379.
- [16] Kasra M and Grynepas M D. On shear properties of trabecular bone under torsional loading: effects of bone marrow and strain rate. *J Biomech.* 2007; 40(13):2898-2903.
- [17] Khor F, Cronin D S, Watson B, Gierczycka D and Malcolm S. Importance of asymmetry and anisotropy in predicting cortical bone response and fracture using human body model femur in three-point bending and axial rotation. *J. Mech. Behav. Biomed. Mater.* 2018; 87:213–229.
- [18] Maheshkumar V. Jadhav and Gambhire V R. Experimental analysis of stress in real (Preserved) intact proximal human femur (Thigh) bone under static load. *IJATES.* 2015 ; 03(1).
- [19] Mathukumar S, Nagarajan V A and Radhakrishnan A. Analysis and validation of femur bone data using finite element method under static load condition. *Proceedings of the*

institution of the mechanical engineers, Part C: Journal of Mechanical engineering science. 2019; 233(16):5547–5555.

- [20] Sina Askarinejad, Joshua E Johnson, Nima Rahbar and Karen L Troy. Effects of loading rate on the mechanical behavior of the femur in falling condition. *J. Mech. Behav. Biomed. Mater.* 2019; S1751-6161:31436.
- [21] Lin Tianye, Yang Peng, Xu Jingli, Wei QiuShi, Zhou GuangQuan, He Wei and Zhang Qingwen. Finite element analysis of different internal fixation method for the treatment of Pauwels type III femoral neck fracture. 2019 ; 112:108658.
- [22] Ali Seker, GokhanBaysal, NafizBilsel and SercanYalcin. Should early weight bearing be allowed after intramedullary fixation of trochanteric femur fractures: A finite element study. *J Orthop Sci.* 2020; 0949-2658.
- [23] Gautam, D., Rao, V.K.P. Nondestructive Evaluation of Mechanical Properties of Femur Bone. *J Nondestruct Eval* 2021; 40, 22.